Photodetachment of hydrogen negative ions with screened Coulomb interaction

Song Bin Zhang,[1] Jian Guo Wang,[2] R. K. Janev,[3] Yi Zhi Qu,[4] and Xiang Jun Chen[1]

[1]*Hefei National Laboratory for Physical Sciences at Microscale and Department of Modern Physics, University of Science and Technology of China, Hefei 230026, People's Republic of China*

[2]*The Key Laboratory of Computational Physics, Institute of Applied Physics and Computational Mathematics, PO Box 8009, Beijing 100088, People's Republic of China*

[3]*Macedonian Academy of Sciences and Arts, PO Box 428, 1000 Skopje, Macedonia*

[4]*College of Material Sciences and Optoelectronic Technology, Graduate School of the Chinese Academy of Sciences, PO Box 4588, Beijing 100049, People's Republic of China*

(Received 5 May 2010; published 28 June 2010)

The effects of Coulomb interaction screening on photodetachment cross sections of hydrogen negative ions below the $n = 2$ excitation threshold is investigated by using the R-matrix method with pseudostates. The contributions of Feshbach and shape resonances to H^- photodetachment cross section are presented when screening length (D) varies from $D = \infty$ to $D = 4.6$ a.u. It is found that the interaction screening has dramatic effects on the photodetachment cross sections of hydrogen negative ions in the photoelectron energy region around the $n = 2$ excitation threshold by strongly affecting the evolution of near-threshold resonances.

DOI: 10.1103/PhysRevA.81.065402 PACS number(s): 32.80.Gc, 52.25.Jm

In many physical systems (dense plasmas, electrolytes, solid-state matter) the Coulomb interaction between the constituent charged particles is screened due to the correlation of many-particle interactions [1–3]. To the lowest particle correlation order (pairwise correlations), the Coulomb interaction screening reduces to the Debye-Hückel (Yukawa-type) potential. For the interaction of an ion of charge Z with an electron it has the form [1–3]:

$$V(r) = -\frac{Ze^2}{r}\exp\left(-\frac{r}{D}\right), \tag{1}$$

where D is the screening length. In a plasma, $D = (k_B T_e/4\pi e^2 n_e)^{1/2}$, with T_e and n_e being the plasma electron temperature and density, respectively, and k_B is the Boltzmann constant.

In the context of hot, dense plasmas studies, a number of theoretical investigations of electron-hydrogen collision processes [4–11] have been carried out by using the interaction (1), while the only study of photodetachment process in such plasmas was done by Kar and Ho [12] for the negative hydrogen ion. Hydrogen negative ions are known to be the principal source of continuous opacity in solar photosphere, and the study of H^- photodetachment in plasmas is of interest due to its presence in the interstellar media [13–15].

In the work of Kar and Ho [12], the H^- photodetachment with screened Coulomb interaction between all three charged particles was described by using the "loosely bound electron" approximation [15,16] for the bound state wave function and a plane wave for the continuum electron wave function. The energy parameter and the normalization constant of initial state (one-electron) wave function were determined with full account of two-electron correlations for each value of considered screening length D. Cross-section results were presented for a large number of screening lengths covering the range from $D = 1$ a.u. to infinity. In the present work we shall treat the H^- photodetachment with screened Coulomb interactions between the charged particles in the form (1) by employing the R-matrix method with pseudostates (RMPS) which allows us to describe the important resonant effects in the process in photoelectron energy regions near the thresholds of excitation channels, and we concentrate on the photoelectron energy region around the $n = 2$ excitation threshold.

The R-matrix method for photon-atom and electron-atom interactions has been discussed in detail by Burke *et al.* [17,18], and we refrain from repeating its description here. The physical orbitals of hydrogen atom with the screened Coulomb potential (1) are calculated by piecewise exact power series expansions of the radial function [19], while the pseudo-orbitals are optimized by the CIV3 computer code [20]. The R-matrix code used in the present work is a modified version based on the Belfast [21,22] atomic R-matrix packages in which the Coulomb interactions in the $(N+1)$-electron nonrelativistic Hamiltonian are replaced by Yukawa-type screened Coulomb interactions (in atomic units):

$$H^{N+1} = \sum_{n=1}^{N+1}\left[-\frac{1}{2}\nabla_n^2 - \frac{Z}{r_n}\exp(-r_n D^{-1}) + \sum_{m>n}^{N+1}\frac{1}{r_{mn}}\exp(-r_{mn}D^{-1})\right], \tag{2}$$

where $\mathbf{r}_n$ is the electron radius vector (with respect to the nucleus Z), $r_{mn} = |\mathbf{r}_m - \mathbf{r}_n|$ is the interelectron distance and D is the screening length. The electron-electron interaction term is expanded as [23]

$$V_{ee} = \frac{\exp(-r_{mn}D^{-1})}{r_{mn}} = \begin{cases} \sum_{l=0}^{\infty}\frac{r_<^l}{r_>^{l+1}}P_l(\cos\theta) & D^{-1} = 0 \\ -D^{-1}\sum_{l=0}^{\infty}(2l+1)j_l(iD^{-1}r_<)h_l^{(1)}(iD^{-1}r_>)P_l(\cos\theta) & D^{-1} > 0 \end{cases}, \tag{3}$$

where $r_> = \max(r_m, r_n), r_< = \min(r_m, r_n)$, P_l, j_l, and $h_l^{(1)}$ are the Legendre polynomials, the spherical Bessel functions and the spherical Hankel functions of the first kind with complex argument, respectively.

In order to determine the basis set for our RMPS calculations in the screened case that ensures convergent results, we first consider the nonscreened case with a basis containing 14 physical states (1*s*-5*s*,2*p*-5*p*,3*d*-5*d*,4*f*,5*f*) and four pseudostates ($6\bar{s}$,$6\bar{p}$,$6\bar{d}$,$6\bar{f}$) in the expansion of the total wave function of the $(N+1)$ electron system. The ground-state energy of H^- was computed to be 0.52645 a.u., about 35 meV higher than the exact one [24], but better than that of the extensive eigenchannel *R*-matrix calculations of Sadeghpour *et al.* [25]. The test calculations show that a larger basis can provide little improvement in the energy value since the configuration interaction (CI) approach used in the *R*-matrix method for the total wave-function expansion cannot efficiently describe the strong two-electron correlation in H^-. The ground-state absolute energy of H^-, excited threshold energies of the H(2*s*) and H(2*p*) states, and variation of resonance positions as a function of the inverse screening length are shown in Fig. 1. The calculated RMPS photodetachment cross sections around the $n = 2$ excitation threshold calculated with the above basis are shown in Fig. 2. The results obtained with the length and velocity gauge for the dipole matrix element differ within 1% and agree very well with the complex-rotation method results of Kuan *et al.* [26] and Lindroth [27]. This test serves as a guide in determining the size of the basis in the calculations with interaction screening.

It should be noted that by checking the convergence of the results for each value of *D*, we obtained the same basis sets given in [10,11] for different groups of *D* values, and the inner boundary was set by the program automatically, where all the wave functions decrease to less than 3×10^{-3}.

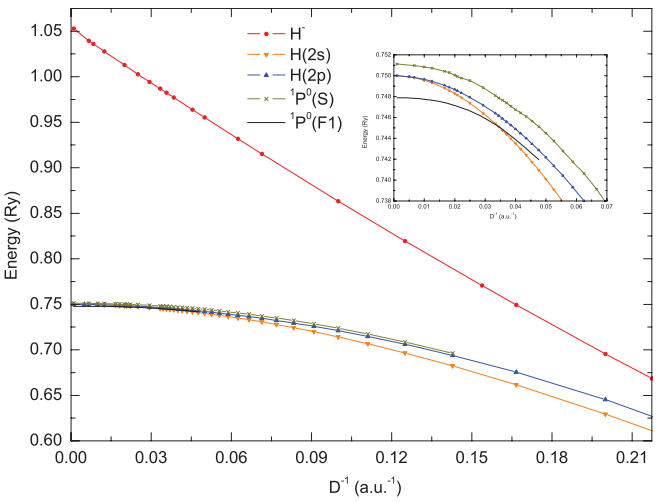

FIG. 1. (Color online) The ground-state absolute energy of H^-, excited threshold energies of the H(2*s*) and H(2*p*) states, and variation of resonance positions as a function of the inverse screening length ($0 \leqslant D^{-1} \leqslant 1/4.6$ a.u.$^{-1}$). Red (dotted) line, H^- ground-state absolute energy; down-triangle line, H(2*s*) excited threshold energy; up-triangle line, H(2*p*) excited threshold energy; cross line, $^1P^\circ$(S) resonance position; black line, $^1P^\circ$(F1) resonance position.

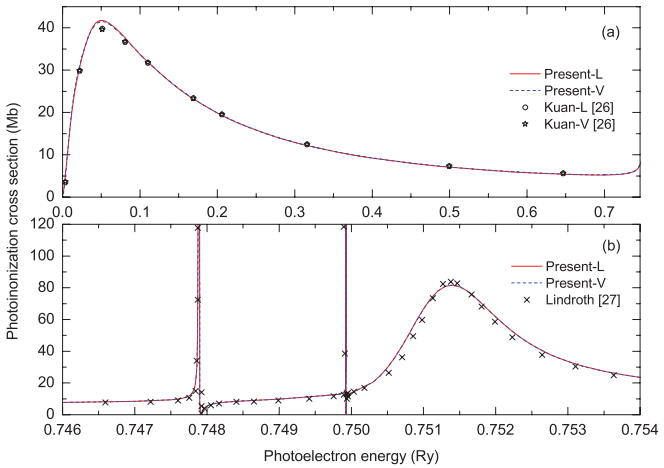

FIG. 2. (Color online) Photodetachment cross sections for the unscreened case around the $n = 2$ excitation threshold. Red line, present RMPS length gauge result; blue (dashed) line, present RMPS velocity gauge result; open circles, length gauge results of Kuan [26]; open stars, velocity gauge results of Kuan [26]; crosses, results of Lindroth [27].

We should also note that when *D* approaches the critical value of $D_{2p} = 4.541$ a.u., the energy of corresponding states becomes increasingly small, the wave functions of the states extend to increasingly large distances, and the backward integration from the asymptotic region toward the inner region becomes increasingly unstable. This results in a practical limit for the lowest value of $D = 4.6$ a.u. in the present calculations.

The dynamical evolution of the photodetachment cross sections for a selected number of screening lengths ranging from $D = \infty$ to $D = 4.6$ a.u. is shown in Fig. 3. The dominant resonances are also marked in the figure [where $^1P^\circ$(Tn) denotes the dominant resonance, *T* stands for the type of the resonance—Feshbach (F) or shape (S) resonance—and *n* for the number of the resonance]. As shown in Fig. 3, the $^1P^\circ$(S) shape resonance gives very large contribution to the photodetachment cross section around $n = 2$ excitation threshold in the entire range of screening lengths considered here. With the decreasing of the screening length *D*, this contribution also decreases. The $^1P^\circ$(F1) Feshbach resonance also plays the important role until *D* decreases to about 20 a.u. Also shown in the figure, the shape of the contribution peak of this resonance changes from an "asymmetric" to a "symmetric" one when *D* passes 30 a.u. This is a consequence of the crossover of $^1P^\circ$(F1) Feshbach resonance to a shape-type resonance in the region around $D \approx 29$–30 a.u., as observed in [10,11]. In contrast to this, the $^1P^\circ$(F2) Feshbach resonance converges to the 2*s* state already at about $D = 120$ a.u. [see Fig. 3(a)]. This is a consequence of the fact that the gradient of the decrease of binding energy of the 2*s* state when *D* decreases is much larger than the one of the $^1P^\circ$(F2) resonance energy position, causing the mixing of the 2*p* state with higher *l* states to be insufficiently strong for transforming a Feshbach resonance into a shape-type resonance [10,11].

The significant changes in the photodetachment cross sections of H^- with the screened Coulomb potential (1) can be appreciated by comparing Fig. 3(a) with Fig. 2(b), covering

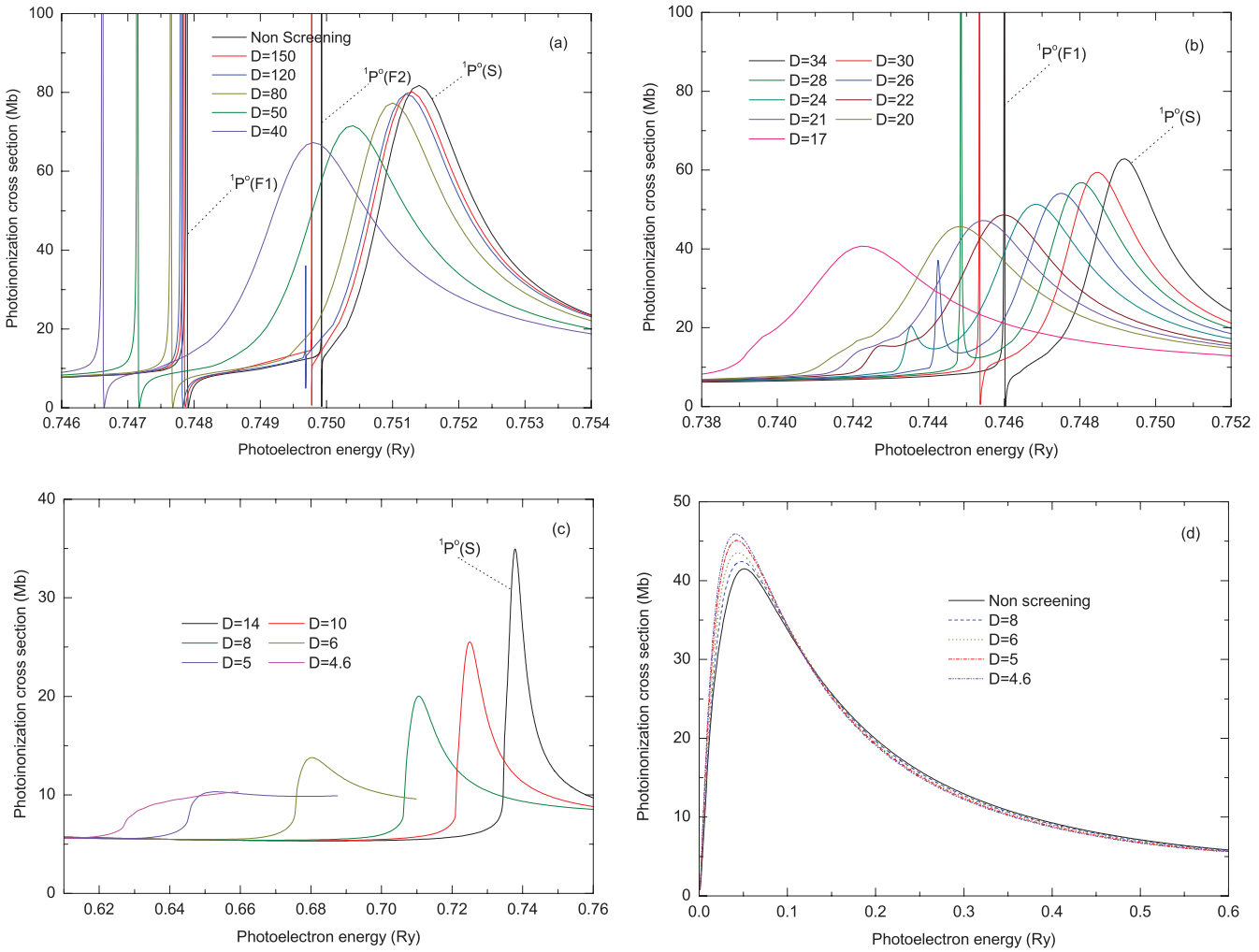

FIG. 3. (Color online) Dynamic evolution of photodetachment cross sections around the $n = 2$ excitation threshold when screening length D decreases from $D = \infty$ to $D = 4.6$ a.u. $^1P^\circ$(Tn) denotes the dominant resonance ($T =$ F, S). (Screening length increases from left to right.)

the same photoelectron energy range. With the decreasing of D, the energy positions of resonances move to a smaller energy region, the widths of Feshbach resonances decrease, and those of shape resonances increase. The transformation of some Feshbach resonances into shape resonances [we have mentioned only that for $^1P^\circ$(F1)] is perhaps one of the most dramatic effects in the interaction screening affecting the photodetachment cross section.

When the photoelectron energy is below 0.62 Ry, far from the $2s$ and $2p$ thresholds, the resonance effects in the photodetachment cross section disappear [as shown in Fig. 3(d)]; the photodetachment cross section normally exhibits a smooth energy dependence behavior for the different value of D. Figure 3(d) shows that with respect to the unscreened case, the photodetachment cross section in the screened case increases with decreasing D for photoelectron energy below about 0.125 Ry, but above this energy it slightly decreases. These properties of the photodetachment cross section are related solely to the behavior of the bound-state electron wave function when D changes. With decreasing D, the maximum of the s-state wave function decreases, while its asymptotic tail increases (see, e.g., [28]). At low energies it is the asymptotic region of the wave function that dominantly determines the value of the dipole matrix element, whereas at high energies the coupling of initial and final state is determined by the bound-state wave function at small distances. In this context we mention that the maxima of the photodetachment cross sections in the work of Kar and Ho [12] for $D = 8$ and 5 a.u. are 4.101×10^{-17} cm^2 and 4.244×10^{-17} cm^2, respectively, while in the present calculations these values are 4.244×10^{-17} cm^2 and 4.509×10^{-17} cm^2, correspondingly. These small differences could be both due to the inapplicability of "loosely bound electron" approximation (employed in [12]) for smaller values of D and the insufficient accuracy of binding energy and bound-state wave function calculated in the present work.

In conclusion, the present study has demonstrated that the screened Coulomb interaction has dramatic effects on the photodetachment cross section of hydrogen negative ions in the photoelectron energy region around the $n = 2$ excitation threshold by strongly affecting the evolution of near-threshold resonances. These effects remain significant even far below the $n = 2$ threshold where the near-threshold resonances do not manifest themselves.

ACKNOWLEDGMENTS

This work was partly supported by the National Natural Science Foundation of China (Grant Nos. 10979007, 10875017, 10774186, and 10876043), the National Key Laboratory of Computational Physics Foundation (Grant No. 9140C6904030808), and the National Basic Research Program of China (Grant No. 2010CB923301).

[1] D. Salzman, *Atomic Physics in Hot Plasmas* (Oxford University Press, Oxford, 1998).
[2] M. S. Murillo and J. C. Weisheit, Phys. Rep. **302**, 1 (1998).
[3] J. P. Hansen and I. R. McDonald, *Theory of Simple Fluids* (Academic, London, 1986).
[4] A. V. Vinogradov and V. P. Shevelko, Sov. Phys. JETP **44**, 542 (1976).
[5] B. L. Whitten, N. F. Lane, and J. C. Weisheit, Phys. Rev. A **29**, 945 (1984); **30**, 650 (1984).
[6] J. K. Yuan, Y. S. Sun, and S. T. Zheng, J. Phys. B **29**, 153 (1996).
[7] Y. D. Jung, Phys. Plasmas **2**, 332 (1995); **2**, 1775 (1995); **4**, 21 (1997).
[8] Y. Y. Qi, Y. Wu, J. G. Wang, and Y. Z. Qu, Phys. Plasmas **16**, 023502 (2009).
[9] Y. D. Jung and J. S. Yoon, J. Phys. B **29**, 3549 (1996).
[10] S. B. Zhang, J. G. Wang, and R. K. Janev, Phys. Rev. Lett. **104**, 023203 (2010).
[11] S. B. Zhang, J. G. Wang, and R. K. Janev, Phys. Rev. A **81**, 032707 (2010).
[12] S. Kar and Y. K. Ho, Phys. Plasmas **15**, 013301 (2008).
[13] R. Wildt, Astrophys. J. **89**, 295 (1939).
[14] S. Chandrasekhar, Astrophys. J. **102**, 223 (1945); **128**, 633 (1958).
[15] A. M. Frolov, J. Phys. B **37**, 853 (2004).
[16] T. Ohmura and H. Ohmura, Phys. Rev. **118**, 154 (1960).
[17] P. G. Burke, A. Hibbert, and W. D. Robb, J. Phys. B **4**, 153 (1971).
[18] P. G. Burke, C. J. Noble, and V. M. Burke, Adv. At. Mol. Opt. Phys. **54**, 237 (2007).
[19] F. Salvat, J. M. Fernfindez-Varea, and W. J. Williamson, Comput. Phys. Commun. **90**, 151 (1995).
[20] A. Hibbert, Comput. Phys. Commun. **9**, 141 (1975).
[21] K. A. Berrington, W. B. Eissner, and P. H. Norrington, Comput. Phys. Commun. **92**, 290 (1995).
[22] Computer code modified version RMATRIX-I, [http://amdpp.phys.strath.ac.uk/rmatrix/].
[23] C. J. Joachain, *Quantum Collision Theory* (North-Holland, Amsterdam, 1975).
[24] C. L. Pekeris, Phys. Rev. **112**, 1649 (1958).
[25] H. R. Sadeghpour, C. H. Greene, and M. Cavagnero, Phys. Rev. A **45**, 1587 (1992).
[26] W. H. Kuan, T. F. Jiang, and K. T. Chung, Phys. Rev. A **60**, 364 (1999).
[27] E. Lindroth, Phys. Rev. A **52**, 2737 (1995).
[28] F. J. Rogers, H. C. Graboske, and D. J. Harwood, Phys. Rev. A **1**, 1577 (1970).